

Experimental investigation on the properties of liquid film breakup induced by shock waves*

Xianzhao Song(宋先钊), Bin Li(李斌)[†], and Lifeng Xie(解立峰)[‡]

School of Chemical Engineering, Nanjing University of Science and Technology, Nanjing 210094, China

(Received 5 March 2020; revised manuscript received 11 May 2020; accepted manuscript online 13 May 2020)

We experimentally observed properties of liquid film breakup for shock-wave-initiated disturbances in air at normal temperature and pressure. The tested liquids include water and various glycerol mixtures. High speed camera and multiple-spark high speed camera were utilized to record the process of liquid film breakup. A phase Doppler particle analyzer was also used to record droplet size and velocity. The experimental results show that liquid viscosity plays a vital role in the deformation, breakup and atomization of liquid films. After the interaction of shock waves, the droplet size of various glycerol mixtures is significantly smaller than either water or glycerol. Richtmyer–Meshkov instability is an important factor in the breakup and atomization of liquid films induced by shock waves. Furthermore, a dispersal model is established to study breakup mechanisms of liquid films. The correlation between droplet size and velocity is revealed quantitatively. The research results may provide improved understanding of breakup mechanisms of liquid films, and have important implications for many fields, especially for heterogeneous detonations of gas/liquid mixtures.

Keywords: shock wave, multiphase flow, Richtmyer–Meshkov instability

PACS: 62.50.–p, 47.55.Ca, 52.57.Fg

DOI: 10.1088/1674-1056/ab928a

1. Introduction

The secondary breakup of liquids is of importance in multiphase flow process with applications to medicine, agriculture, military, combustion instability of sprays, heterogeneous detonations of gas/liquid mixtures, the properties of rain, and interactions between high-speed aircraft and raindrops. Due to numerous applications, secondary breakup has received significant attention from researchers.^[1–3] Pilch and Erdman^[4] predicted the maximum size of stable fragments for acceleration-induced breakup of a liquid drop by velocity history data. Hsiang and Faeth^[5–7] found the mechanism of drop deformation and breakup. Dumouchel^[8] reported the internal geometrical nozzle characteristics and internal flow details that influence the atomization mechanisms. Chauvin *et al.*^[9] studied the secondary atomization induced by shock waves numerically and experimentally. Yao *et al.*^[10] investigated the characteristics of gas-liquid Taylor flow with different liquid viscosities in a rectangular microchannel. It was found that increasing glycerol concentration led to more stable flow, as well as a shortened squeezing stage in a formation cycle. Liang *et al.*^[11] studied deformation and breakup of single drop in laminar and transitional jet flows. The results show that critical capillary and Weber numbers for drop breakup can be estimated based on the mean flow velocity and mean deformation, which are 0.2 and 30, respectively, for this particular flow system. The breakup characteristics of aqueous droplet with surfactant in oil under direct current electric field were inves-

tigated by Luo *et al.*^[12] The results show that the presence of surfactant reduces the steady deformation of droplet and significantly decelerates the stretching process, resulting from the redistribution of surfactant molecules within the oil/water interface. Recently, Liao *et al.*^[13] conducted an experiment using a free-falling drop tower facility for drop dynamic studies in liquid flow. It was found that this method has the particular advantage of conducting the drop deformation and breakup experiments with low density ratio. However, most of the earlier research focused on the single droplet rather than a liquid film. When a liquid film is broken into a lot of droplets, it could be seen as a droplet group. The breakup mechanism of the droplet group is a complex process. Therefore, it is necessary to investigate properties of liquid film breakup induced by shock waves.

The definition and conditions for the onset of various regimes of secondary breakup have been investigated by researchers. The regimes of secondary breakup are often divided into vibrational, bag, multimode, sheet-thinning, and catastrophic.^[4,5] Many researchers have found that the Weber number We and the Ohnesorge number Oh are the main factors influencing the regimes. According to this theory, the transition Weber number between surfactant-laden drop bag breakup and shear breakup of secondary atomization was investigated by Zhao *et al.*^[14] The data show that the predicted expression of the transition Weber number is close to the experimental results. Furthermore, most investigations were fo-

*Project supported by the Young Scientists Fund of the National Natural Science Foundation of China (Grant No. 11802136) and the Young Scientists Fund of the National Natural Science Foundation of China (Grant No. 11802136).

[†]Corresponding author. E-mail: libin@njust.edu.cn

[‡]Corresponding author. E-mail: xielifeng319@sina.com

cused on droplet breakup at low Oh number of moderate We number, so more work about high Oh number is needed.

The aerosol fuel clouds containing droplets may burn faster than an optimally homogeneous vapor/air mixture.^[15–19] Many studies have been performed to regard the droplet size and combustion characteristics of liquid fuels.^[20,21] Liu *et al.*^[22] investigated the influence of droplet size on the explosion parameters of n -hexane/air mixture. The results show that the minimum ignition energy (MIE) of the two-phase vapor-liquid n -hexane is positively correlated with the Sauter mean diameter (SMD). With the SMD values of 10.63 μm and 18.51 μm , the MIEs of n -hexane/air mixtures are 0.5 mJ and 2 mJ, respectively. Therefore, in order to further understand the heterogeneous detonations of gas/liquid mixtures, it is necessary to study the droplet size distribution induced by shock waves.

In order to explore the effect of liquid viscosity on liquid film breakup induced by shock waves, water and various glycerol mixtures are chosen as the liquid samples in this study. Furthermore, droplet size distribution and droplet velocity are obtained experimentally, and these values are quantified. The breakup mechanism of liquid films is discussed. Furthermore, a dispersal model is established by the experimental data.

2. Experimental details

2.1. Experimental setup

The experiments were carried out by a vertical steel tube with the height of 1.0 m and inner diameter of 32 mm. The experimental system consists of a shock wave generating system and measurement systems, as shown in Fig. 1.

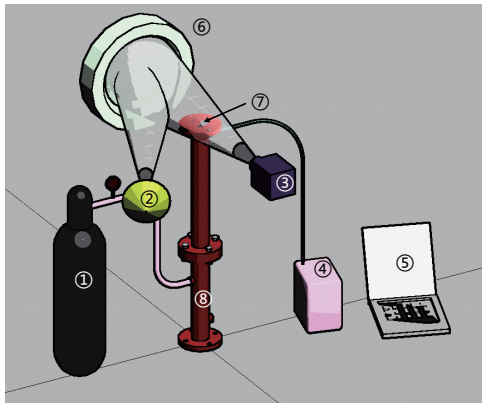


Fig. 1. The image of experimental layout: (1) gas cylinder; (2) light source; (3) camera; (4) pressure testing system; (5) computer; (6) concave mirror; (7) liquid sample; (8) shock tube.

The shock wave generating system includes a compressed air container, a shock wave tube and diaphragms. The shock wave tube consists of a high-pressure section with the height of 0.3 m and a low-pressure section with height of 0.7 m. In the experiment, the diaphragm was set up between the high-pressure section and low-pressure section. The diaphragm was

hard paper film and the thickness of the single layer film was 0.12 mm. The high-pressure section of the shock wave tube was filled up with the high-pressure air. When the air pressure in high-pressure section was over the limitation of diaphragm, the diaphragm would be broken into a hole and meanwhile a shock wave with certain intensity would be generated. Steel wire mesh with a mesh number of 200 was used to hold liquid samples at the top of the shock wave tube. The liquid samples can be held horizontally on the steel wire mesh. The shape of the liquid film was not affected obviously by liquid viscosity and surface tension.

The measurement system consists of three parts. The first is the pressure testing system, which was used to detect the intensity of shock waves using the time difference and distance data of the two pressure measuring points. The second is multiple-spark high speed camera, which was used to capture the whole interaction process and to record the velocity and dispersal area of droplets. The third is a phase doppler particle analyzer (PDPA) used to record velocities and diameters of liquid samples after the interaction of shock waves, and the systematic structure diagram is depicted in Fig. 2.

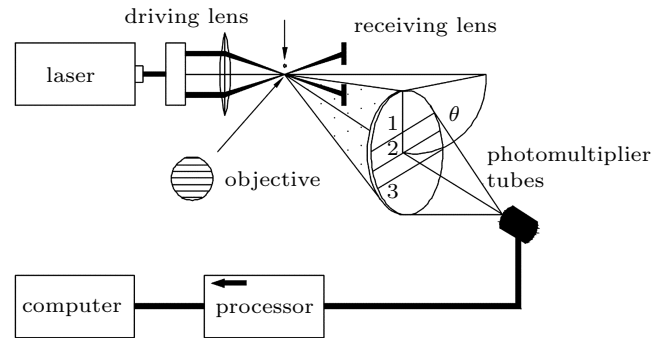


Fig. 2. Systematic structure diagram of phase doppler particle analyzer.

Test samples including water and various glycerol mixtures were used to provide an extensive range of viscosities in this study. Combined to the previous researches,^[4,5] the column liquid film in this study was regard as a spherical liquid drop. However, diameter/thickness ratios in this experiment were too large, the equivalent diameter needed to be corrected. According to formulas between the ellipsoid volume and the sphere volume in the equivalent volume method, the corrected liquid film equivalent diameters listed in Table 1 are obtained based on the actual diameter deviation within 10%. Parameters of liquid samples are given in Table 2. Properties of air are taken at normal temperature and pressure: $\rho_G = 1.18 \text{ kg/m}^3$, $\mu_G = 18.5 \times 10^{-6} \text{ kg/ms}$.

We , Oh , T are dimensionless parameters used to describe flow state in the actual interaction and dispersal processes. These definitions are as follows:^[4]

$$We = \frac{\rho V^2 D}{\sigma}, \quad (1)$$

where V is the relative velocity of gas and liquid states; D is the diameter of liquid droplet; ρ is the density of gas; σ is the surface tension of liquid sample.

$$Oh = \frac{\mu_d}{(\rho_d D \sigma)^{0.5}}, \quad (2)$$

where μ_d is the viscosity coefficient of liquid; ρ_d is the density of liquid.

$$T = t \frac{Ve^{0.5}}{D}, \quad (3)$$

where e is the density ratio of gas and liquid, and t is the actual time.

In this test, We varied from 5531.62 to 29010.27, Oh varied from 0.001 to 2.72, and ρ_L/ρ_G varied from 845 to 1068.

Table 1. Calculated diameters of liquid samples.

Thickness of liquid samples/mm	Equivalent diameter/mm	Corrected equivalent diameter/mm
2	7.3	2.7
4	9.2	5.3
6	10.5	8.0
8	11.5	10.6
10	12.4	12.4

Table 2. Parameters of liquid samples.

Liquid materials	$\rho/(\text{kg} \cdot \text{m}^{-3})$	$\mu_L/(10^{-4} \text{ kg} \cdot \text{m}^{-1} \cdot \text{s}^{-1})$	$\sigma/(10^{-3} \text{ N} \cdot \text{m}^{-1})$
Water	997	8.94	70.8
Glycerol	1260	12500	62.0
30% glycerol	1081	253	64.2
50% glycerol	1134	66	65.2
70% glycerol	1181	24	66.5

2.2. Experimental procedures

Before the experiment, samples were injected by a syringe on the steel wire mesh uniformly. Then the valve of gas cylinder was opened. Meanwhile, multiple-spark high speed camera captured the whole interaction process. Changing the variation of the numbers of diaphragms can get different intensities of shock waves. The average value of Mach numbers was measured by pressure transducers before official experiments. The measured results are given in Table 3. Table 4 shows the dimensionless parameters of glycerol films under different Mach numbers.

Ambient temperature was 20 °C and the pressure was 101 kPa during experiment procedures. The thickness of liquid samples was kept from 2 mm to 10 mm with steps of 2 mm. The thickness of diaphragm decided the Mach number of shock waves.

Table 3. The Mach numbers of shocks in the blank test.

Number of Diaphragms	Average value of shock wave velocity/(m/s)	Average value of Mach number
1	524	1.54
2	588	1.73
3	612	1.80

Table 4. The dimensionless parameters of glycerol films under different Mach numbers.

Mach number	Thickness/mm	We	Oh	Re
1.54	2.7	6316.75	2.72	838.90
	5.3	12399.55	1.94	1646.73
	8.0	18716.30	1.58	2485.63
	10.6	24799.10	1.37	3293.45
	12.4	29010.27	1.27	3852.72
1.73	2.7	12298.93	2.72	1262.85
	5.3	24142.34	1.94	2478.92
	8.0	36441.27	1.58	3741.76
	10.6	48284.69	1.37	4957.84
	12.4	56483.97	1.27	5799.73
1.80	2.7	15071.95	2.72	1432.57
	5.3	29585.68	1.94	2812.08
	8.0	44657.64	1.58	4244.66
	10.6	59171.37	1.37	5624.17
	12.4	69219.33	1.27	6579.22

3. Results and discussions

3.1. Blank test

In order to adjust the whole system and provide comparison data with formal experiments, blank tests were carried out. In the blank tests, no liquid samples were put on the steel wire mesh. Figure 3 shows that the shock wave generated by vertical shock tube was a spherical wave and its wave front was so smooth. There was a small turbulent area like a mushroom cloud at the center of Fig. 3. The reason for this phenomenon is that the steel wire mesh was filled at the exit of the shock tube. Although there were dense holes in the steel wire mesh, the shock wave was strong enough to transmit through it, and the diffraction and reflection would cause the flow field in this area to be disordered and to form a turbulent area. Researchers^[23] have illustrated that the wire mesh tends to enhance the mixing process. However, this phenomenon was no longer obvious after adding liquid samples during the formal experiment and the main objective of this study was to explore the interaction between shock waves and liquid samples, so the effect of steel wire mesh could be ignored.

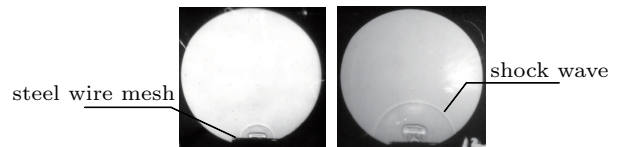


Fig. 3. Experimental photos of shock waves in blank test using YA-16 multiple-spark high speed camera (without liquid samples).

3.2. Breakup mechanism of liquid film

According to the breakup mechanism,^[4] the liquid film breakup belongs to catastrophic breakup because the weber numbers (shown in Table 4) are all greater than 350 in this study. There are significantly differences for water films and glycerol films in the atomization and dispersal process, as shown in Fig. 4. Firstly, the water film is much larger than the glycerol film in the zone of atomization and dispersal, which is

obvious from the picture at 2400 μs . Secondly, water droplets and glycerol droplets move at a similar speed in the vertical direction, while the horizontal velocity of water droplets is significantly higher than that of glycerol droplets, which also causes dispersal zone of the water film to be larger than the dispersal zone of the glycerol film. The main reason for this phenomenon is that the physical properties of water and glycerol are greatly different, mainly in the dynamic viscosity coefficient. The viscosity of water is much smaller than that of glycerol, so it is easier to break into small droplets after shock

wave action, and it is not easy to re-polymerize. The effect of breakup and atomization after shock waves is obvious. The water droplets are spread to the surroundings due to aerodynamic force, surface tension, gravity and air drag force. However, the glycerol droplets generated by the breakup are larger due to the fact that the glycerol is more viscous, and the main droplet group still moves to the vertical direction under the action of aerodynamic force, only a few tiny glycerol droplets have a tendency to move to the horizontal direction.

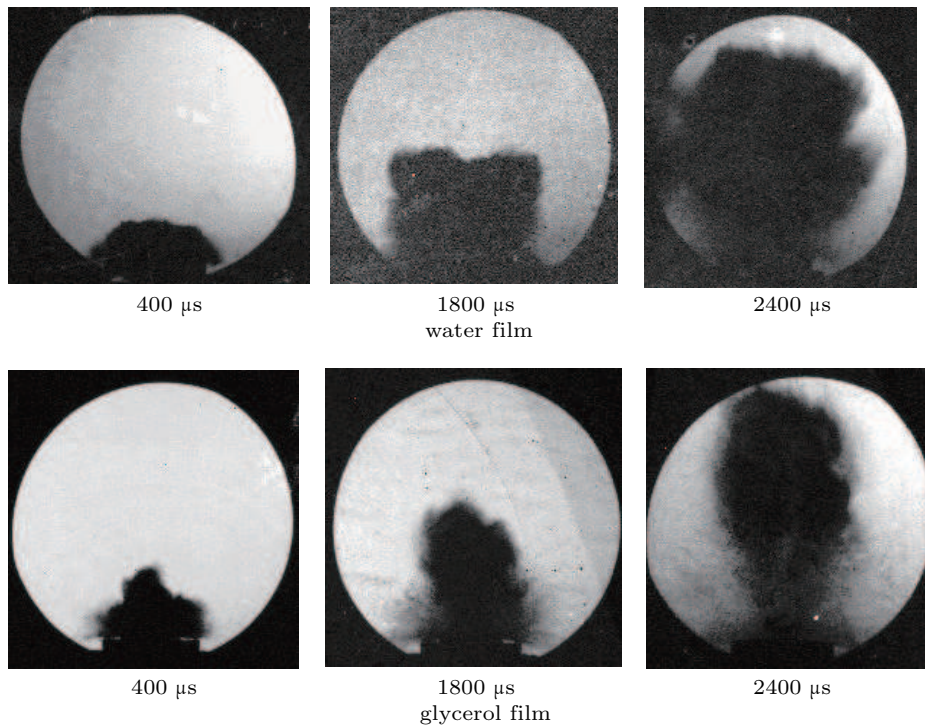


Fig. 4. Water film and glycerol film after the interaction of shock waves ($Ma = 1.73$).

Figure 5 shows the breakup of the glycerol film with thickness of 10 mm and different Mach numbers. With the increase of the Mach number, in the initial stage of the action, the glycerol film is gradually enlarged from a tiny point protrusion in the film center ($Ma = 1.54$) to an apparent surface protrusion ($Ma = 1.8$). The formed cloud is also transformed from a well-defined T shape to a dispersed “mushroom” shape. After processing the image, it is found that the dispersal height and width for shock waves with the Mach number of 1.8 are about 2.5 times and 1.5 times higher than those of shock waves with Mach number of 1.54, respectively. The atomization effect of the glycerol film for shock waves with the Mach number of 1.8 is the best, so aerodynamic force is still in a dominant position in the whole process of dispersion and cloud formation. Therefore, breakup and atomization effects of glycerol droplets become better with the increasing Mach number. These results further support the idea of previous observations (e.g., You *et al.*^[24] in 2017).

Figure 6 shows the process of shock wave traveling across the liquid samples, including crossing interface 1 (from high pressure gas to liquid) and interface 2 (from liquid to air). This process is similar to the phenomena of liquid explosive dispersing, which has been investigated for many years due to its widely applications in industry fields and military areas (e.g., fuel–air explosion). Some researchers thought that the liquid dispersing flow is a typical liquid–gas two-phase flow of multi-scales in space and time. According to the assumption that (a) the liquid is homogeneous after the interaction of shock waves, (b) the liquid flow is inviscid, incompressible, adiabatic and irrotational, (c) the liquid expands in radial direction and forms a continuous shell, Gardner^[25] put forward a linear thin liquid shell instability model (see Fig. 7(a)). In our experiments, it means that there are perturbations with smaller amplitudes of perturbation than the thickness of a liquid film at the initial state on the interface 1 and interface 2. As the amplitude of perturbation on interfaces is larger than the thickness of liquid

film, the liquid film may break up. In addition, Samirant^[26] obtained photos of the liquid shell by using x-ray photographic technology, which may support the model of Gardner (see Fig. 7(b)).

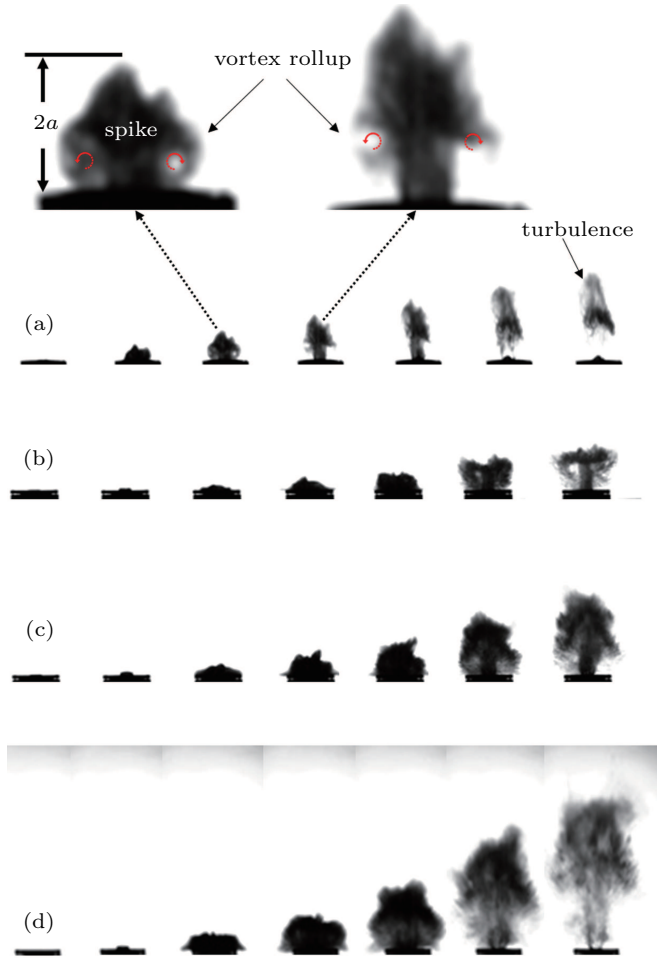


Fig. 5. Breakup of the glycerol film induced by shock waves with different Mach numbers. (a) $Ma = 1.54$, thickness = 2 mm, (b) $Ma = 1.54$, thickness = 10 mm, (c) $Ma = 1.73$, thickness = 10 mm, (d) $Ma = 1.8$, thickness = 10 mm.

Furthermore, the Richtmyer–Meshkov instability (RMI)^[27,28] is that the interface is always unstable both in the case of shock wave passage from the lighter gas to the heavier one and in the case from opposite direction, which is different from the RTI in Refs. [29–31], where the interface is unstable only when the lighter fluid accelerates the heavier one. The RMI is modelled as follows:

$$a(t) = a_0(1 + kA\Delta Vt), \quad (4)$$

where a is the growth of the perturbation amplitude, k is the wavenumber of the initial disturbance, ΔV is the velocity change of the interface due to impulsive acceleration, and A is the Atwood number defined by

$$A = \frac{\rho_1 - \rho_2}{\rho_1 + \rho_2}, \quad (5)$$

with ρ_1 being the density of heavier fluids and ρ_2 the density of lighter fluids.

In the generation of RMI, a disturbed interface is subjected to an impulsive acceleration (usually produced by shock waves), which deposits kinetic energy on the fluid interface and causes the disturbance to grow with time. This growth ultimately causes the fluids separated by the interface to mix together and becomes turbulent, as shown in Fig. 5(a). This instability is initiated by baroclinic vorticity deposition and the two-dimensional inviscid vorticity transport equation is depicted as follows:^[32]

$$\rho \frac{D}{Dt} \left(\frac{\omega}{\rho} \right) = \frac{1}{\rho^2} \nabla \rho \times \nabla P, \quad (6)$$

where ∇P is a pressure gradient, $\nabla \rho$ is a density gradient, and ω is the vorticity.

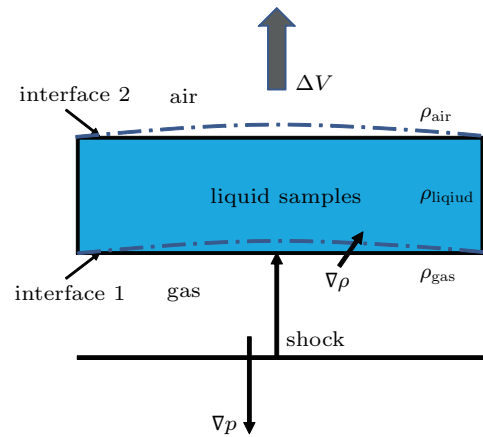


Fig. 6. The shock wave travels upward and toward the interface and applies a pressure gradient across the density gradient.

When there are misalignments of pressure and density gradients, the initial vorticity (ω) distribution will be generated by shock waves. Huete *et al.*^[33] found that additional weak vorticity would also be generated by the transmitted and reflected shock waves, which would be curved due to interaction with the perturbed interface. The deposited vorticity causes the interface to roll up into mushroom-like spikes of heavy fluid penetrating into the light fluid, as shown in Fig. 5. All the numbers of vorticities deposited by the shock wave decide the growth rate of the instability. With the growth of the spikes and bubbles, the vorticity rolls up into regions of concentrated vorticity of alternating sign. The growth of a secondary instability appears due to the rolling up of the vorticity, which would generate shear on the thin arms of the mushroom structure. Finally, the secondary instability becomes turbulent. Turbulence is a complex process. Therefore, it is indicated that RMI is an important factor in the breakup and atomization of liquid films.

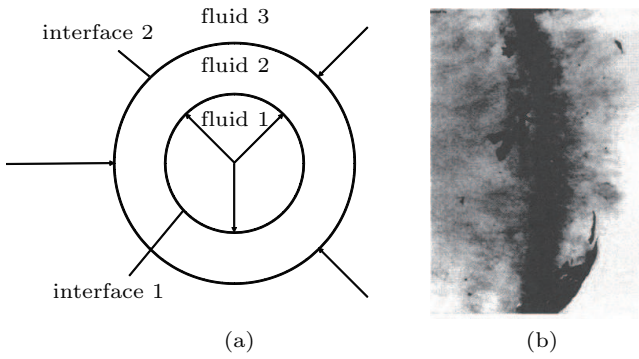


Fig. 7. (a) A linear thin liquid shell instability model proposed by Gardner, (b) liquid shell in expansion from Samirant by flash x-ray photograph.

3.3. Droplet size distribution

It is important to address droplet size distributions after secondary breakup, because this affects the details needed to characterize properties of secondary breakup and correlations of droplet size and velocity.

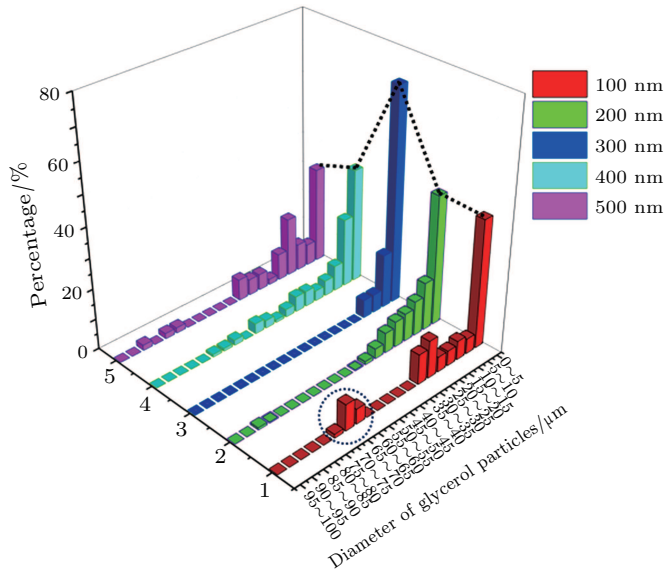


Fig. 8. Diameter of Glycerol droplets formed in zones with 5 kinds of distances from the exit of shock tube (thickness of liquid samples = 2 mm, $Ma = 1.54$).

There are 5 external measuring points in the axial line with the shock tube to capture the parameters of liquid samples, such as droplet size and velocity. The distances of measuring points from the outlet of shock tube are kept from 100 mm to 500 mm with a step of 100 mm. The resulting droplet size distributions of glycerol (thickness = 2 mm, $Ma = 1.54$) are illustrated in Fig. 8. Perhaps the most striking feature of Fig. 8 is that the diameter range of glycerol droplets formed under perfect conditions is below 90 μm , and diameters of most droplets are between 0 μm and 35 μm , approximately 90%. With the increase of distance, the percentage of droplet size below 5 μm increases firstly and then decreases, and the maximum value appears at the distance of 300 mm. Meanwhile, the percentage of droplet size between 60 μm and

75 μm significantly reduces with the distance increasing to 300 mm and then slightly grows. It is indicated that mother droplets are broken into small droplets with the distance increasing to 300 mm, which is also referred to as the process of secondary atomization. The direction of droplet motion is uncertain, so the probability of collision between droplets is large. Therefore, small droplets are recombined into large droplets within the dispersal process. These results show that the glycerol droplets face an obvious breakup after the interaction of shock waves.

Figure 9 shows that the average diameter of glycerol is significantly larger than that of water with the Mach number of 1.73, and the average of the difference between them is 9.62 μm . The reason is that the viscous force of glycerol is too large to easily form dispersed micro droplets compared to water. However, when the thickness of the liquid film is 9 mm, droplet sizes of them are almost the same. The shock wave needs to consume more energy on the liquid film to support the deformation and breakup with the increase of the thickness of the liquid film. With the increasing thickness of the liquid film, the Weber number We increases, and the Ohnesorge number Oh decreases, which mean that drag force increases and liquid viscous force decreases. These results are in agreement with Hsiang and Faeth (1992)^[5] who also found that droplets would deform and break up at $We > 1$, with the following deformation and breakup regimes (depicted in order of appearance with adding We at $Oh < 0.1$): no deformation, nonoscillatory deformation, oscillatory deformation, bag breakup, multimode breakup and shear breakup, indicating that droplet deformation and breakup become more violent with the increase of We . Thus, it is prone to produce much smaller droplets when the thickness of the liquid film increases.

Average diameter of liquid samples with different thicknesses ($Ma = 1.73$) is depicted in Fig. 10. It is obvious that the droplet size of various glycerol mixtures after the interaction of shock waves is significantly smaller than either water or glycerol. The reason is that the van der Waals force exists not only between water molecules and water molecules, but also between glycerol molecules and glycerol molecules, and more likely exists between water molecules and glycerol molecules. Planchette *et al.*^[34] found that, because no free water is available at the investigated glycerol concentration, glycerol, which is also a co-solvent, may additionally modify long-range interactions by reducing van der Waals attractions or giving rise to repulsive surface-solvent mediated forces of entropic origin. In this case, the van der Waals force of the mixture is significantly smaller than those between droplets of pure water or pure glycerol (99.5%). Thus, various glycerol mixtures are more likely to be deformation and breakup, producing more small droplets.

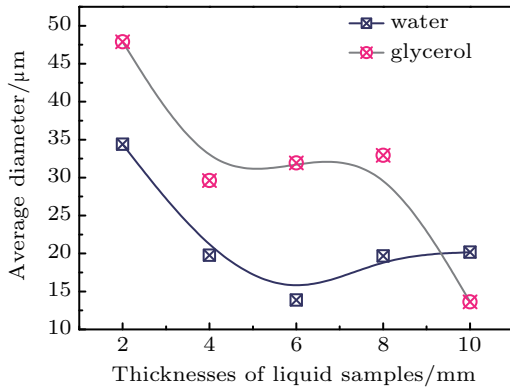


Fig. 9. Average diameter of the liquid samples with different thicknesses ($Ma = 1.73$).

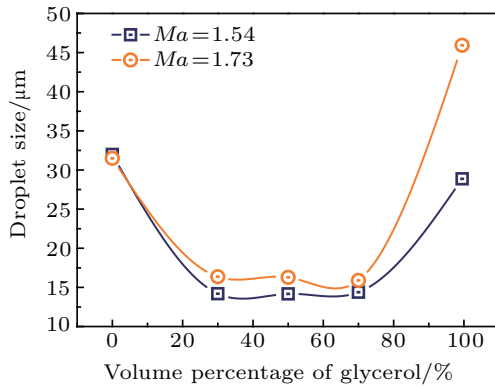


Fig. 10. Droplet size with volume percentage of glycerol.

3.4. Droplet velocity

Figures 11 and 12 show that the average vertical velocity of droplets is significantly greater than the average horizontal velocity because the aerodynamic force is always the dominant force. At the same time, due to the instability of the flow field after interaction of shock waves, the law of vertical motion velocity under different thicknesses of liquid films is not obvious. Generally, when the shock wave overcomes the gravity, surface tension and viscous force of the liquid film, the vertical velocities of water films and glycerol films are relatively close. When the liquid film is thin, it is not easy for glycerol film to generate small droplets due to its high viscous. At this time, more kinetic energy may be obtained as a whole, and the vertical velocity is faster. However, because the water film is easier to break up, the energy is not obtained enough, so that the vertical velocity is small. The regularity of horizontal velocity variation is basically the same as that of vertical velocity variation. As the thickness of liquid film increases, a minimum value appears at the thickness of 5 mm, which may be due to the fact that the viscous force and surface tension of the liquid film and the aerodynamic force reach a balance in the horizontal direction under this condition. Most of the droplets move in the direction of the shock wave after the dispersion, and the directionality is relatively uniform, so that the horizontal velocity is small.

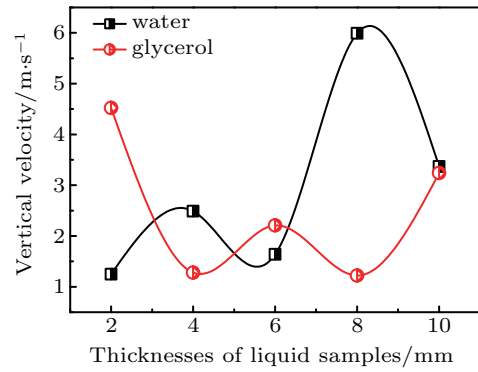


Fig. 11. Vertical velocity with different thicknesses of liquid samples ($Ma = 1.73$).

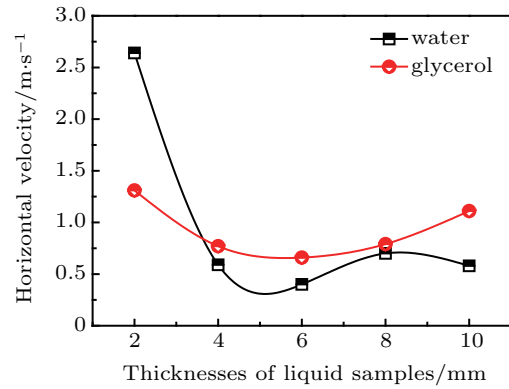


Fig. 12. Horizontal velocity with different thicknesses of liquid samples ($Ma = 1.73$).

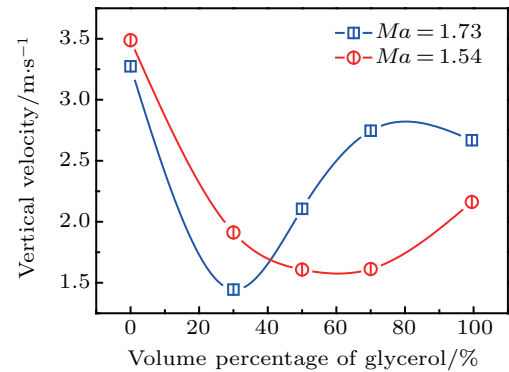


Fig. 13. Vertical velocity with different volume percentages of glycerol (thickness of liquid film = 2 mm).

Figures 13 and 14 show that with the increase of glycerol content, both the vertical velocity and horizontal velocity first decrease and then increase. In the case of pure water, the horizontal velocity obtained under the effect of aerodynamic force is large since the density and mass of water are small, and when the glycerol content is increased, the horizontal velocity of droplets has a decreasing process. When the glycerol content is 30% and the Mach number is 1.73, the horizontal velocity of droplets reaches the lowest value, which may result from the state of the liquid film after breakup is the most unstable condition, resulting in instability of the movement state of droplets.

Due to the low density of water molecules, the initial movement velocity obtained by aerodynamic force is signif-

icantly larger than that of glycerol molecules, and it is less affected by gravity and air resistance, so it is easy to maintain a high velocity of movement. This is also the reason why vertical velocity of droplets is large when the glycerol content is low. When the glycerol content is about 30% and the Mach number is 1.73, both the vertical velocity and horizontal velocity are small.

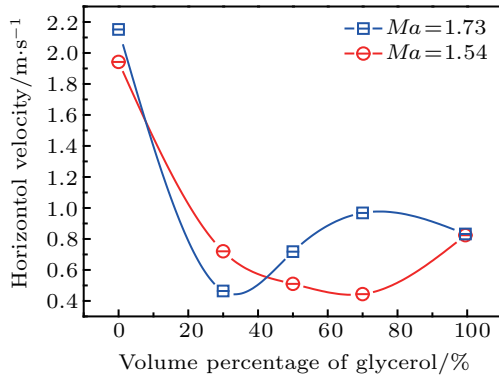


Fig. 14. Horizontal velocity with different volume percentages of glycerol (thickness of liquid film = 2 mm).

3.5. Droplet size/velocity correlation

Based on the PDPA measurement results, the model of the droplet size and velocity of droplets formed by the interaction of shock waves is established.

Statistical Product and Service Solutions (SPSS), a common statistics software, is used to establish the model equation. Taking We , Oh and φ (volume fraction of water in the mixture) as the dependent variables and D_{50} (the mean drop diameter), V_h (horizontal velocity) and V_v (vertical velocity) as independent variables, the model equation is fitted as:

$$D_{50} = 370.769 + 0022We - 26.871We^{0.3} - 31.442Oh + 126.034Oh^{0.3} - 65.632\varphi, \quad (7)$$

$$V_h = 83.457 + 0005We - 6.124We^{0.3} - 31.071Oh + 93.161Oh^{0.3} - 42.126\varphi, \quad (8)$$

$$V_v = 34.125 + 0002We - 1.926We^{0.3} - 12.235Oh + 38.976Oh^{0.3} - 19.619\varphi. \quad (9)$$

The correlation coefficient R^2 for Eq. (7) is 0.982 and the significance character $\text{Sig} = 0.005$, which indicates the model equation could explain 98.2% of the experimental data and the independent variables play obvious roles on the dependent variables. The correlation coefficient R^2 for Eq. (8) is 0.934 and the significance character $\text{Sig} = 0.018$, which means that the model equation could explain 93.4% of the experimental data and the independent variables play important roles on the dependent variable. The correlation coefficient R^2 for Eq. (9) is 0.877 and the significance character $\text{Sig} = 0.058$, which means that the model equation can explain 87.7% of the experimental results. However, since the value of Sig exceeds the

set confidence interval of 0.05, this model expression could be used to characterize and calculate the vertical velocity of the droplet, while more data are needed for further fitting.

It can be seen from the model that φ is inversely proportional to D_{50} , V_h , and V_v , which is consistent with the previous analysis results. Furthermore, the model can be used to predict the relationship between the droplet size and velocity of liquid film breakup and to provide detailed data reference for heterogeneous ignition.

3.6. Model analysis

There is a high contrast on the dynamic viscosity parameters between water and glycerol. As an important factor determining the Oh number of the dimensionless parameter of the flow field, the difference of the dynamic viscosity parameters would have an important impact on the process of liquid dispersion under the action of aerodynamic force. Aiming at this phenomenon, it is of great significance to establish a liquid-spraying model driven by shock waves.

Taking We , Oh , and T as the dependent variables and D_h (horizontal dispersion distance) and D_v (vertical dispersion distance) as independent variables and using 750 sets of data (partial data are listed in Table 5), the model equation is fitted as follows:

$$D_h = -341.117 + 3.133We^{0.3} - 51.12Oh^{0.3} + 3.861T - 234.683T^{0.5} + 507.505T^{0.3}, \quad (10)$$

$$D_v = -519.506 + 11.576We^{0.3} - 27.002Oh^{0.3} - 24.84T + 348.009T^{0.5} - 157.578T^{0.3}. \quad (11)$$

The correlation coefficient R^2 for Eq. (10) is 0.839 and the significance character $\text{Sig} < 0.01$, which means that the model equation could explain 83.9% of the experimental results and the independent variables play obvious roles on the dependent variable. The correlation coefficient R^2 for Eq. (11) is 0.915 and the significance character $\text{Sig} < 0.001$, which means that the model equation can explain 91.5% of the experimental results and the independent variables play obvious roles on the dependent variable.

Based on the value of significance character, it is obvious that the results of vertical-dispersion distance are significantly better than those of the horizontal one. This is mainly because the aerodynamic force moves in the vertical direction during the liquid film breakup, so the vertical dispersion distance is mainly affected by the aerodynamic force. The results of vertical-dispersion distance are more uniform. However, the uniformity of the horizontal dispersion distance is relatively poor due to the fact that the horizontal dispersion distance is mainly determined by aerodynamic force, gas-liquid interface instability and air drag force.

Table 5. Partial data of parameters in the experiments.

Liquid materials	We	Oh	T	D_h/mm	D_v/mm
Water	5531.62	0.002	2.233673	10	15
Water	10858.36	0.0015	1.137909	12	12
Water	16389.98	0.0012	0.753865	15	8
Water	21716.73	0.001	0.568954	15	6
Water	25404.47	0.001	0.486364	15	5
Water	10770.25	0.002	3.116781	9	15
Water	21141.60	0.0015	1.587794	11	14
30% Glycerol	5889.3032	0.005448	2.145133	7	14
30% Glycerol	11560.484	0.003888	1.092804	9	11
30% Glycerol	17449.787	0.003165	0.723982	11	8
30% Glycerol	23120.968	0.002749	0.546402	12	6
30% Glycerol	27047.17	0.002542	0.467085	12	5
30% Glycerol	11466.671	0.005448	2.993236	8	14
30% Glycerol	22508.651	0.003888	1.524856	9	16
50% Glycerol	6006.7279	0.014772	2.094405	6	14
50% Glycerol	11790.984	0.010543	1.066961	7	11
50% Glycerol	17797.712	0.008582	0.706862	9	7
50% Glycerol	23581.969	0.007455	0.53348	9	5
50% Glycerol	27586.454	0.006893	0.45604	9	5
50% Glycerol	11695.301	0.014772	2.922452	6	14
50% Glycerol	22957.443	0.010543	1.488796	7	13
70% Glycerol	6100.2906	0.055917	2.052306	5	13
70% Glycerol	11974.645	0.039911	1.045515	6	11
70% Glycerol	18074.935	0.032485	0.692653	8	7
70% Glycerol	23949.289	0.028221	0.522757	8	5
70% Glycerol	28016.15	0.026093	0.446873	8	4
70% Glycerol	11877.471	0.055917	2.863709	4	13
70% Glycerol	23315.035	0.039911	1.458871	6	13
Glycerol	6316.75	2.72	1.986927	3	13
Glycerol	12399.55	1.94	1.012208	4	10
Glycerol	18716.3	1.58	0.670588	6	7
Glycerol	24799.1	1.37	0.506104	6	5
Glycerol	29010.27	1.27	0.432637	6	4
Glycerol	12298.93	2.72	2.772481	4	12
Glycerol	24142.34	1.94	1.412396	4	11

4. Conclusions

We have studied the properties of liquid film breakup induced by shock waves, considering water and various glycerol mixtures in air at normal temperature and pressure (We of 5531.62–29010.27, Oh of 0.001–2.72, ρ_L/ρ_G of 845–1068). The major conclusions are as follows:

(1) Liquid viscosity has a great influence on the deformation, breakup and atomization of liquid film, which increases significantly with the Ohnesorge number Oh .

(2) Richtmyer–Meshkov instability is an important factor in the breakup and atomization of the liquid film induced by shock waves.

(3) Droplet size distribution and droplet velocity have been revealed by experimental data. In particular, after the in-

teraction of shock waves, the droplet size of various glycerol mixtures is significantly smaller than either water or glycerol.

(4) To further study breakup mechanism of liquid films, droplet size/velocity correlation and model analysis have been established. It can be used to predict the droplet size and velocity of liquid film breakup under different conditions.

References

- [1] Guildenbecher D R, Lopez-Rivera C and Sojka P E 2009 *Exp. Fluids* **46** 371
- [2] Qian L J and Lin J Z 2011 *Sci. Chin.-Phys. Mech. Astron.* **54** 2109
- [3] Wang J, Ruan W J, Wang H and Zhang L L 2019 *Chin. Phys. B* **28** 064704
- [4] Pilch M and Erdman C A 1987 *Int. J. Multiph. Flow* **13** 741
- [5] Hsiang L P and Faeth G M 1992 *Int. J. Multiph. Flow* **18** 635
- [6] Hsiang L P and Faeth G M 1993 *Int. J. Multiph. Flow* **19** 721
- [7] Hsiang L P and Faeth G M 1995 *Int. J. Multiph. Flow* **21** 545
- [8] Dumouchel C 2008 *Exp. Fluids* **45** 371
- [9] Chauvin A, Daniel E, Chinnayya A, Massoni J and Jourdan G 2016 *Shock Waves* **26** 403
- [10] Yao C, Zheng J, Zhao Y, Zhang Q and Chen G 2019 *Chem. Eng. J.* **373** 437
- [11] Liang W, Wang D, Cai Z, Li Z, Huang X, Gao Z, Derksen J J and Komrakova A E 2019 *Chem. Engin. J.* **386** 121812
- [12] Luo X, Yan H, Huang X, Yang D, Wang J and He L 2017 *J. Colloid Interface Sci.* **505** 460
- [13] Liao B, Zhang G F, Zhu Y J, Li Z F, Li E Q and Yang J M 2018 *Sci. Chin.-Phys. Mech. Astron.* **61** 104721
- [14] Zhao H, Wu Z W, Li W F, Xu J L and Liu H F 2018 *Fuel* **221** 138
- [15] Bowen P J and Cameron L R J 1999 *Process Saf. Environ. Protect.* **77** 22
- [16] Jackson S, Lee B J and Shepherd J E 2016 *Combust. Flame* **167** 24
- [17] Yoshida K, Hayashi K, Morii Y, Murakami K, Tsuboi N and Hayashi A K 2016 *Combust. Sci. Technol.* **188** 2012
- [18] Zhang B and Liu H 2019 *Fuel* **258** 116132
- [19] Zhang B, Liu H, Yan B and Hoi Dick N 2020 *Fuel* **259** 116220
- [20] Hu E, Tian H, Zhang X, Li X and Huang Z 2017 *Fuel* **188** 90
- [21] Liu X, Wang Y and Zhang Q 2016 *Fuel* **165** 279
- [22] Liu X, Zhang Q and Wang Y 2015 *Process Saf. Environ. Protect.* **95** 184
- [23] Prasad J K, Rasheed A, Kumar S and Sturtevant B 2000 *Phys. Fluids* **12** 2108
- [24] You Z M, Li B, Wang H Y and Xie L F 2017 *J. Aerosol. Sci.* **106** 100
- [25] Gardner D R 1990 *Technical Report: Near-field dispersal modeling for liquid fuel-air explosives* (U.S. Department of Energy Office of Scientific and Technical Information OSTI.GOV)
- [26] Samirant M 1999 *Prevention of Hazardous Fires and Explosions* (Berlin: Springer) Chap. 26 pp. 123–134
- [27] Meshkov E E 1972 *Fluid Dyn.* **4** 101
- [28] Richtmyer R D 1960 *Commun. Pure Appl. Math.* **13** 297
- [29] Taylor G I 1950 *Proc. R. Soc. London A* **201** 192
- [30] Rayleigh 1882 *Proc. London Math. Soc.* **s1–14** 170
- [31] Zhai Z G, Zou L Y, Wu Q and Luo X S 2018 *Proc. Inst. Mech. Eng. Part. C-J. Eng. Mech. Eng. Sci.* **232** 2830
- [32] Morgan R V, Aure R, Stockero J D, Greenough J A, Cabot W, Likhachev O A and Jacobs J W 2012 *J. Fluid Mech.* **712** 354
- [33] Huete R d L C, Velikovich A L and Wouchuk J G 2011 *Phys. Rev. E* **83** 056320
- [34] Planchette C, Mercuri A, Arcangeli L, Kriechbaum M and Laggner P 2017 *AAPS PharmSciTech.* **18** 3053